Progress In Electromagnetics Research C, Vol. 54, 163–169, 2014

A Fully Planar Near-Field Resonant Parasitic Antenna

Sen Yan* and Guy A. E. Vandenbosch

Abstract—A near-field resonant parasitic (NFRP) antenna is presented. Unlike the conventional NFRP antenna, which is fed by coaxial cables, the topology is driven by a planar "monopole". In this way, the antenna and the front end circuit can be designed in a single plane, which is crucial for system integration. The radiator is electrically small ($\lambda_0/19.3 \times \lambda_0/10.47 \times \lambda_0/76.4$) while reaching a high efficiency (94%) and a good bandwidth (85 MHz). The operating frequency and input impedance are easily tailored. Measured results verify the working mechanism.

1. INTRODUCTION

Electrically Small Antennas (ESAs) are applied abundantly in modern communication systems [1–3]. A lot of methods have been studied to reduce the size of an antenna. Among others, this resulted in planar inverted-F antennas (PIFA), meander transmission line antennas loaded microstrip antennas, and surface mounted device (SMD) loaded antennas [4–9]. In the last decade, the use of metamaterials (MMs) also has shown to have potential to miniaturize antennas. It has been proven that a shell of ideal homogenous MM can reduce the antenna size, while keeping a high efficiency [10–15]. However, in practise a homogenous MM is hard to obtain, since the typical size of the MM unit cell is about 10% of the wavelength in vacuum.

The NFRP antennas proposed by Ziolkowski solve this problem [16]. In a NFRP antenna, the homogenous MM shell is replaced by a single MM unit cell. The radiation of the whole system is mainly generated by the currents in this unit cell, which is driven by the near field of a very small radiator feed. By changing the coupling between the driver and the radiating structure, the input impedance of the antenna can be adjusted to fit to a 50 Ω feeding line. A matching network is unnecessary, which is helpful to minimize the size of the antenna. Several designs have been proposed that show a good performance [17–21]. However, most of these antennas are driven by small vertical monopoles, and fed by coaxial cables. These small monopoles are perpendicular to a large PEC plane connected with the ground. Since this geometry is not planar, it is difficult to integrate with frond end circuits. A large ground plane is usually undesirable in integrated systems, and a "vertical" feeding of the antenna brings difficulties for the fabrication.

In this paper, we introduce a new type of NFRP antenna, which is driven by a planar or "horizontal" monopole, without compromising the small antenna size and the high efficiency. Thanks to this new feeding type, the antenna reaches a high level of omnidirectionality. Since it is fed by a microstrip line, the topology can be kept fully planar, which allows to fabricate it very cheap on a printed circuit board (PCB). This is very attractive for application in mobile communications, e.g., Bluetooth, Wifi, GSM, etc.. It also opens the possibility to use this type topology in Body Area Networks, where vertical feeds are rather incompatible with on-body integration.

In Section 2 the configuration of the proposed antenna is presented in detail. In Section 3, the physical parameters are studied in order to show how to control the resonant frequency and input impedance of the antenna. A prototype is fabricated and measured in Section 4. A brief conclusion is given in Section 5.

Received 28 August 2014, Accepted 12 October 2014, Scheduled 5 November 2014

* Corresponding author: Sen Yan (sen.yan@esat.kuleuven.be).
The authors are with the ESAT-TELEMIC, KU Leuven, Kasteelpark Arenberg 10, Leuven B-3001, Belgium.

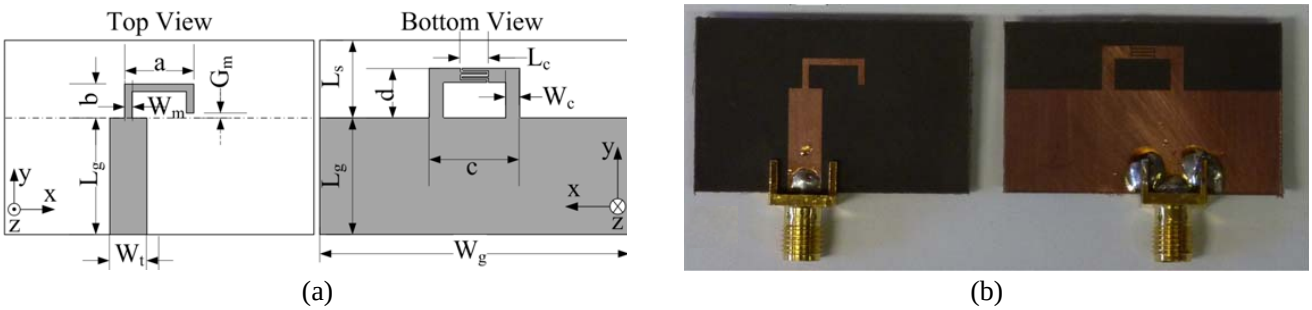

Figure 1. (a) Configuration of the antenna, width of he fingers: W_d, gap between the fingers: G_d. (b) Antenna prototype.

Table 1. Dimensions of the proposed antenna. (Unit: mm).

a	b	W_m	G_m	c	d	W_c
8.99	4.31	0.96	0.59	11.74	6.38	1.83
L_c	W_d	G_d	L_s	L_g	W_g	W_t
3.62	0.29	0.22	10	15	40	4.85

2. ANTENNA CONFIGURATION

The topology is shown in Figure 1(a). The substrate is Rogers RT/duroid 5880 ($\varepsilon_r = 2.2$, $\tan\delta = 0.0009$, thickness 1.575 mm). A small bent monopole is fed by a 50 Ω microstrip line directly. As the monopole is electrically extremely small, it shows a small input resistance. A capacitively-loaded loop (CLL) is located on the ground plane. An interdigital capacitor is used to obtain a large capacitance value. At resonance, this capacitance is neutralized by the inductance due to the current path formed by the CLL structure and the ground plane. So, the CLL structure is a self resonant reactive element which is driven by the bent monopole [16]. This helps to reduce the total size of the antenna. By tuning the coupling between the bent monopole and the CLL structure, good impedance matching can be obtained without extra matching network.

The CLL controls the working frequency of the antenna. The working frequency decreases with increasing CLL length or capacitor value. The latter can be implemented by increasing the number of fingers, increasing the length of the fingers, or reducing the gap width in between the fingers. The length and width of the monopole can also be tuned to obtain impedance matching. A photo of the design, which is covering the full 2.4 GHz WLAN band, is shown in Figure 1(b) and Table 1. Its performance will be discussed in Section 4.

3. ANALYSIS OF INPUT IMPEDANCE

Figure 2 displays the input impedance of the antenna simulated with CST MWS. Three different situations are considered: small monopole without CLL, small monopole with CLL, CLL fed by the microstrip line directly. At the working frequency, the monopole is too small compared with the wavelength, so it does not resonate and cannot radiate energy efficiently. Its input impedance is nearly zero and its radiation efficiency is very low. Its first resonance appears at 4.04 GHz, where the length of the monopole is about a quarter wavelength. The CLL fed by the microstrip line directly shows a strong high Q resonance at about 4.16 GHz, with high impedance values. This reduces the bandwidth significantly. The input resistance is too high to be fed by the 50 Ω transmission line directly, and an additional matching network is needed. Only the small monopole loaded with the CLL shows an acceptable input impedance at about 2.44 GHz, and can be connected to the feeding line directly. It is worth to mention that the working frequency is lower than the resonant frequency of the CLL.

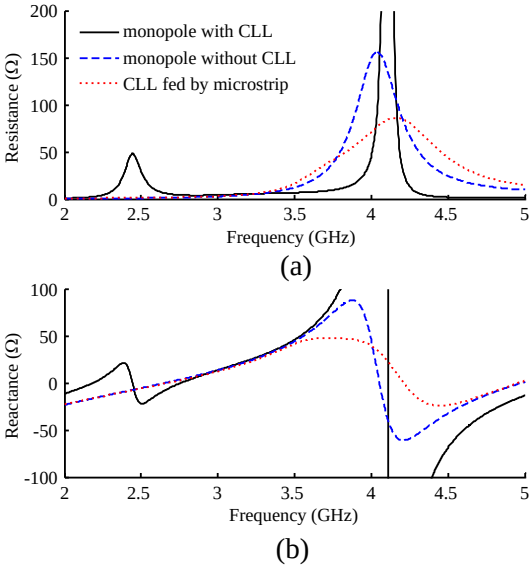

Figure 2. Simulated input impedance of the antenna in Figure 1. (a) Real part. (b) Imaginary part.

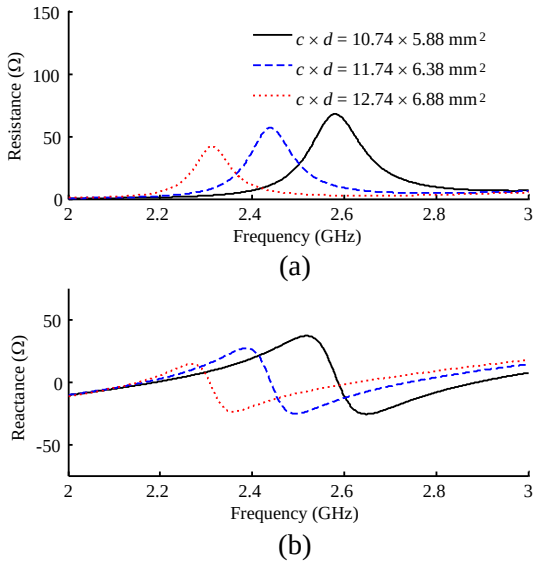

Figure 3. Simulated input impedance for different lengths of the interdigital capacitor loop. (a) Real part. (b) Imaginary part.

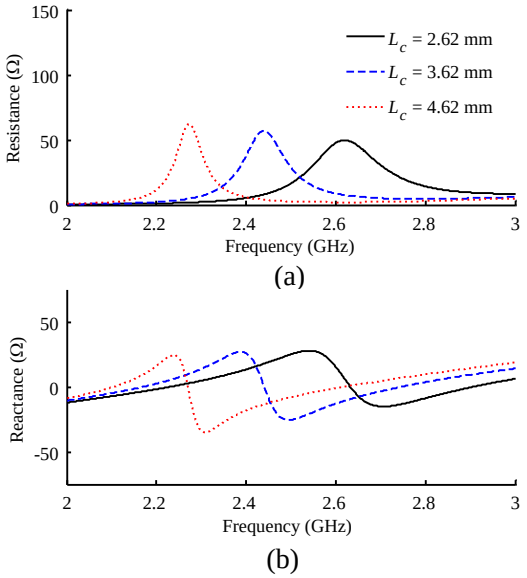

Figure 4. Simulated input impedance for different lengths of the CLL fingers. (a) Real part. (b) Imaginary part.

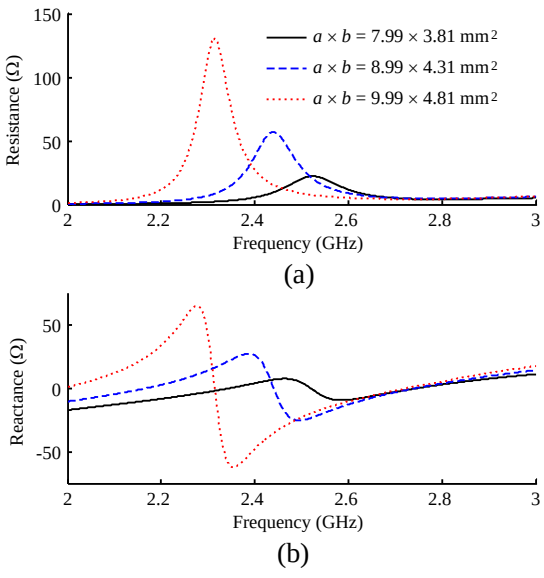

Figure 5. Simulated input impedance as a function of length of the bent monopole. (a) Real part. (b) Imaginary part.

This means that the CLL is not working as a separate resonant unit, but is strongly coupled to the feeding structure. Another interpretation is that it serves as a parasitic unit to "change the effective permeability of the surroundings" near the monopole.

The change of the input impedance with the most important physical parameters was also investigated. In Figure 3, the length of the interdigital capacitor loop is increased while the other parameters are kept the same (see Table 1). The larger inductance due to the longer length of the CLL loop leads to a lower resonant frequency. Figure 4 shows the results for a changing length of the CLL. Longer fingers will bring a larger capacitance, so the resonant frequency also shifts to lower

frequencies. Note that changing either the inductance or capacitance will influence the input impedance of the antenna. To obtain impedance matching, the driven monopole should be tuned. Figure 5 shows the results for three bent monopoles with different lengths. As the length of the monopole increases, the resonant frequency shifts to lower frequencies and the input resistance increases sharply. By adjusting the length of the monopole and the CLL, it is easy to design an antenna that is matched at the desired frequency.

4. RESULTS

The reflection coefficient of the fabricated prototype is shown in Figure 6. The measured and simulated S_{11} agree well, except for a very little frequency shift. The antenna shows a measured bandwidth (S_{11} below -10 dB) of about 83 MHz around 2.44 GHz. The minimum return loss is below -42 dB. It has to be emphasized that the good matching is obtained without additional impedance transformer.

Figure 7 depicts the radiation pattern of this NPRF antenna. Since it is a small antenna, eventhough the topology of the antenna is not symmetric, a quasi-symmetric omnidirectional radiation pattern can be observed. That is extremely suitable for wireless communications. There is a little difference between simulated and measured radiation patterns. This may be due to the feeding cable which can influence the radiation. The maximum beam direction appears in the y direction, and the realized gain is about 3.0 dB in both the simulation and measurement. Table 2 lists some important performance parameters of the antenna. The total efficiency calculated by the Wheeler cap method [22] is larger than 94%. Considering the size of the radiator, i.e., without the ground plate, is $\lambda_0/19.3 \times \lambda_0/10.47 \times \lambda_0/76.4$, and with the ground plate is $\lambda_0/3.08 \times \lambda_0/4.92 \times \lambda_0/76.4$ the total efficiency is relatively high.

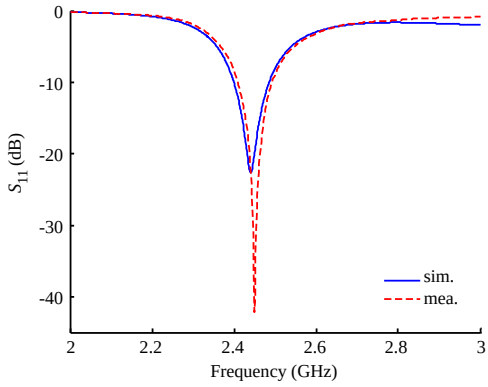

Figure 6. Simulated and measured reflection coefficient.

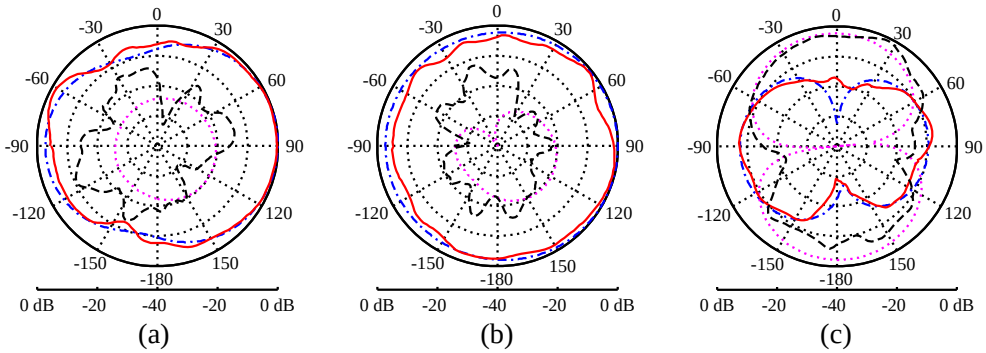

Figure 7. Simulated and measured radiation pattern at 2.45 GHz. (a) x-y plane, (b) y-z plane, (c) x-z plane. The orientation of the antenna is the same as in Figure 1. (blue dashbot line: simulated φ component, red solid line: measured φ component, magenta dotted line: simulated θ component, black dashed line: measured θ component).

Table 2. Comparison of simulated and measured performance.

	Freq. (GHz)	S_{11} (dB)	BW (MHz)	Dir. (dB)	Gain (dB)	Eff. (%)
Simulated	2.441	−22.6	86	3.24	3.04	95.6
Measured	2.45	−42.2	84	/	3.02	94.2

Table 3. Comparison of several ESAs in literature.

Ref.	Freq. (GHz)	BW (%)	ka	Dir. (dB)	Eff. (%)	Planar	Feeding
Design 8 in [16]	1.577	1.27	0.492	3.66	76.8	no	coaxial
Design 11 in [16]	1.576	0.90	0.417	3.58	78.2	no	coaxial
[17]	0.305	0.24	0.268	4.3	17.5	no	coaxial
Figure 1 in [21]	0.289	0.69	0.434	3.86	82.3	no	coaxial
[20]	1.578	4.56	0.845	1.54	73.8	yes	coaxial
7	2.45	4.45	0.23	3.5	69	yes	Microstrip
9	2.44	9.1	0.835	2.1	83	yes	coaxial
This paper	2.441	3.48	0.344	3.24	95.6	yes	Microstrip

*k is the free space wavenumber and a is the radius of the smallest sphere enclosing the entire antenna system.

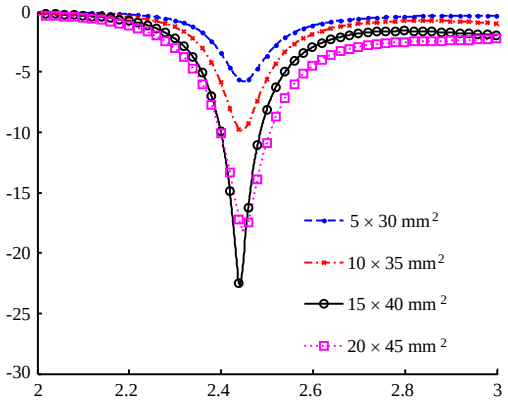

Figure 8. Reflection coefficient as a function of size of ground ($L_g \times W_g$).

It is also interesting to study the effect of the size of the ground for this kind of antenna. Figure 8 shows the calculated S_{11} for several antennas with different ground sizes. It is clearly seen that the position of the resonant frequency is not influenced by the size of the ground, but the level of the reflection is changed. A minimum ground should be kept for a good matching. When the size of the ground is smaller than $10 \times 35\,\text{mm}^2$, no $-10\,\text{dB}$ matching bandwidth is observed. For larger grounds, the bandwidth increases with increasing size of the ground, reaching a maximum at a ground size of $20 \times 35\,\text{mm}^2$. Further increasing the ground size does not further increase the bandwidth significantly.

In Table 3, several ESAs (Electrically Small Antennas) from literature are compared. The first five antennas are based on the NFRP concept. The radiators proposed in [16, 17, 21] have nearly the same size. However, our antenna is the only one that has a totally planar structure. These designs include a large ground plane perpendicular to the monopoles. Also, the bandwidth of our antenna is considerably larger compared to most antennas in the table. The antenna in [20] also has a planar topology and the largest bandwidth. However, it is significantly larger than all other designs in the table, and its feeding is still realized by a vertical coaxial probe. This is not suited for integration with planar circuits. The antenna in [7] is a small slot antenna loaded with SMD capacitors. The antenna is extremely compact

but its efficiency is low due to the losses in the SMD components. [9] proposes a kind of miniaturized Hilbert inverted-F antenna. Its bandwidth is relatively wide at the cost of a significantly bigger size. Note also that our antenna has the highest efficiency in the table. Efficiency is also the main issue with the miniature size antennas sometimes used for Bluetooth applications.

5. CONCLUSION

An NFRP antenna is presented in this paper. The whole antenna is fabricated on a printed circuit board without vias. Since the antenna is driven by a planar monopole, the large metal ground plane perpendicular to the antenna can be removed, so front-end circuits can be connected with the antenna by a microstrip line directly in the same plane. This is very practical for system integration. The advantages of the antenna are its small size ($\lambda_0/19.3 \times \lambda_0/10.47 \times \lambda_0/76.4$), and its high efficiency (94%). Both simulated and measured results verify the working mechanism.

REFERENCES

1. Garg, R., P. Bhartia, I. Bahl, and A. Ittipiboon, *Microstrip Antenna Design Handbook,* Artech House, 2001.
2. Wong, K. L., *Compact and Broadband Microstrip Antennas,* Wiley, 2002.
3. Anguera, J., A. Andújar, M. C. Huynh, C. Orlenius, C. Picher, and C. Puente, "Advances in antenna technology for wireless handheld devices," *International Journal on Antennas and Propagation*, Vol. 2013, Article ID 838364, 2013.
4. Soh, P. J., G. A. E. Vandenbosch, O. L. Soo, and N. H. M. Rais, "Design of a broadband all-textile slotted PIFA," *IEEE Trans. Antennas Propag.*, Vol. 60, No. 1, 379–384, Jan. 2012.
5. Sallam, M. O., E. A. Soliman1, G. A. E. Vandenbosch, and W. D. Raedt, "Novel electrically small meander line RFID tag antenna," *International Journal of RF and Microwave Computer-Aided Engineering*, Vol. 23, No. 6, 639–645, 2012.
6. Radiom, S., H. Aliakbarian, G. A. E. Vandenbosch, and G. G. E. Gielen, "An effective technique for symmetric planar monopole antenna miniaturization," *IEEE Trans. Antennas Propag.*, Vol. 57, No. 10, 2989–2996, Oct. 2009.
7. Wang, Y.-S. and S.-J. Chung, "A short open-end slot antenna with equivalent circuit analysis," *IEEE Trans. Antennas Propag.*, Vol. 58, No. 5, 1771–1775, Oct. 2010.
8. Ban, Y.-L., J.-J. Chen, S.-C. Sun, J. L.-W. Li, and J.-H. Guo, "Printed wideband antenna with chip-capacitor loaded inductive strip for LTE/GSM/UMTS WWAN wireless USB dongle applications," *Progress In Electromagnetics Research*, Vol. 128, 313–329, 2012.
9. Huang, J.-T., J.-H. Shiao, and J.-M. Wu, "A miniaturized Hilbert inverted-F antenna for wireless sensor network applications," *IEEE Trans. Antennas Propag.*, Vol. 58, No. 9, 3100–3103, Sep. 2010.
10. Ziolkowski, R. W. and A. Eipple, "Application of double negative metamaterials to increase the power radiated by electrically small antennas," *IEEE Trans. Antennas Propag.*, Vol. 54, 2113–2130, Jul. 2006.
11. Stuart, H. R. and A. Pidwerbetsky, "Electrically small antenna elements using negative permittivity resonators," *IEEE Trans. Antennas Propag.*, Vol. 54, No. 6, 1644–1653, Jun. 2006.
12. Chen, P. Y. and A. Alu, "Sub-wavelength elliptical patch antenna loaded with μ-negative metamaterials," *IEEE Trans. Antennas Propag.*, Vol. 58, No. 9, 2909–2919, Sep. 2010.
13. Ahmadi, A., S. Saadat, and H. Mosallaei, "Resonance and Q performance of ellipsoidal ENG subwavelength radiators," *IEEE Trans. Antennas Propag.*, Vol. 59, No. 3, 706–713, Mar. 2011.
14. Alici, K. B., A. E. Serebryannikov, and E. Ozbay, "Radiation properties and coupling analysis of a metamaterial based, dual polarization, dual band, multiple split ring resonator antenna," *Journal of Electromagnetic Waves and Applications*, Vol. 24, Nos. 8–9, 1183–1193, 2012.
15. Choia, J. and S. Lim, "Frequency and radiation pattern reconfigurable small metamaterial antenna using its extraordinary zeroth-order resonance," *Journal of Electromagnetic Waves and Applications*, Vol. 24, Nos. 14–15, 2119–2127, Apr. 2012.

16. Erentok, A. and R. W. Ziolkowski, "Metamaterial-inspired efficient electrically small antennas," *IEEE Trans. Antennas Propag.*, Vol. 56, No. 3, 691–701, Mar. 2008.
17. Kim, O. S. and O. Breinbjerg, "Miniaturised self-resonant split-ring resonator antenna," *Electronics Letters*, Vol. 45, No. 4, 196–197, Feb. 2009.
18. Ziolkowski, R. W., P. Jin, and C.-C. Lin, "Metamaterial-inspired engineering of antennas," *Proceedings of the IEEE*, Vol. 99, No. 10, 1720–1731, Oct. 2010.
19. Quevedo-Teruel, O., M. N. M. Kehn, and E. Rajo-Iglesias, "Dual-band patch antennas based on short-circuited split ring resonators," *IEEE Trans. Antennas Propag.*, Vol. 59, No. 8, 2758–2765, Aug. 2011.
20. Jin, P. and R. W. Ziolkowski, "Multi-frequency, linear and circular polarized, metamaterial-inspired, near-field resonant parasitic antennas," *IEEE Trans. Antennas Propag.*, Vol. 59, No. 5, 1446–1459, May 2011.
21. Jin, P. and R. W. Ziolkowski, "Multiband extensions of the electrically small, near-field resonant parasitic Z antenna," *IET Microw. Antennas Propag.*, Vol. 4, No. 8, 1016–1025, 2010.
22. Pozar, D. M. and B. Kaufman, "Comparison of three methods for the measurement of printed antenna efficiency," *IEEE Trans. Antennas Propag.*, Vol. 36, No. 1, 136–139, Jan. 1988.